JAST, Vol. 4, No. 1, pp 9–16


JAST
Journal of Aerospace Science and Technology

# Numerical Analysis of the Influence of Stopping Holes in the Crack Growth

**M. R. Khoshravan[1], A. Hamidi[2]**

*Fracture and crack growth of mechanical structures is a usual phenomenon caused by application of tensile, cyclic loading or thermal stresses on the structure. Therefore, introducing methods for preventing the crack growth is useful. One method for repairing crack growth, consisting of making a hole in the crack tip to eliminate the sharp corners is explained. This method is frequently used in air and space industry. Drilling can be done in various locations; however, for our study three locations in the crack tip for the hole are considered. In the first, the hole is situated in the left of the crack tip (Location A). In the second, it is sited in the center of the crack tip (Location B) and in the last it is located in the right side of the crack tip (Location C). The study of resistance against crack growth is based on the comparison of these three systems. We have analyzed the influence of these stopping holes, their diameters and their locations on the fracture toughness. The specimens were made of Al 7075-T6 alloy, and had the shape of the Compact Tension specimen. The solicitation was a monotonic tensile loading in the Mode I fracture. The stress intensity factor and the critical load versus the crack length of the test bars were computed. Numerical analysis was carried out with a finite element method using Ansys software. Following this numerical analysis, fracture experimentation was carried out on the tensile machine to evaluate the influence of the stopping hole on the critical load for initiation of the crack growth. Results show that the best location of the hole could increase the critical load by 54% and the location which gave the weakest result showed 11% of increase in the load. Thus, based on this research, the best location of the stopping hole and its diameter were found to increase the life span of mechanical pieces.*

## NOMENCLATURE

| | |
|---|---|
| $a$ | Crack length |
| $B$ | Thickness of specimen |
| $E$ | Young's modulus |
| $f_{ij}^{\alpha}(\theta)$ | Function of $\theta$ |
| $F$ | Correction factor |
| $K$ | Stress intensity factor |
| $K_{\alpha}$ | Parametrical stress intensity factor near crack tip |
| $K_{IC}$ | Critical stress intensity factor in plane strain |
| $K_C$ | Critical stress intensity factor in plane stress |
| $P_{cr}$ | Critical load |
| $R$ | Radius of hole |
| $r$ | Radius of the plastic zone |
| $W$ | Width of specimen |
| $\alpha$ | Shape factor |
| $\nu$ | Poisson ratio |
| $\sigma$ | Stress |
| $\sigma_{ij}$ | Parametrical stress near crack tip |
| $\sigma_{\max}$ | Maximum stress |
| $\partial\sigma/\partial x$ | Stress gradient at notch |

1. *Assistant Professor, Dept. of Mech. Eng., Tabriz Univ., Tabriz, Iran, Email: rkhosh@tabrizu.ac.ir.*
2. *MSc. Student, Dept. of Mech. Eng., Tabriz Univ., Tabriz, Iran, Email: aydin2020@yahoo.com*

$\sigma_u$ Ultimate stress

$\sigma_y$ Yield stress

## INTRODUCTION

Initiation of a crack and its growth in the aeronautical structures and pieces are inevitable phenomena. Applied cyclic loads, shrinkage due to welding, thermal stress and so on are the main causes of crack growth. Thus, introducing repairing methods could be useful. In the aerospace industry, creation of stopping holes at the crack tip is of special importance.

Experimental studies concerning the role of stopping holes were carried out in metallic structures, especially in the metallic bridges [1,2]. Also research concerning the repair of cracks by introducing stopping holes in the aerospace industry has been carried out. Most often after 4000 hours of flying, some cracks appeare in different parts of a plane or helicopter. In the zone of the door, after drilling the crack tip and adhesion of reinforcing plates, the growth of the crack is stopped. Also for stopping the hole in the cabin zone, drills with diameters of 2.5mm are used [3]. Cracks shorter than 4 inches appearing in stator of the disc of turbine and compressor are drilled with a diameter of 3 mm [4].

In all of these studies, generality of repairing by stopping holes is represented, but the location of the stopping hole at the crack tip and its diameter is not discussed. Qi [5] has studied different locations of stopping holes. He proposes that diameters of stopping holes should be 10 to 15 percent of the crack length to obtain efficiency of the hole in stopping the crack growth. Dirikolu *et.al.* [6] have studied stress intensity ($K$) near the stopping holes with different diameters in composite materials. Investigations concerning the position of the stopping hole in industrial application are done [7,8]. Results show that the strain which originally causes the crack is concentrated at the crack tip and tends to extend the crack. Therefore, a small hole, with a 1/8" drill bit, was drilled at the crack tip to distribute the strain over a wider area. Each crack occurring at any hole or tear was drilled in the same manner.

Some numerical analyses were carried out in this field. Chen *et.al.* [9] analyzed some parts of airplane structure made of Al7075-T6 and Al2024-T3. They used DCB and MT specimen. The values of their stress-strain curve were used in our research. In the results of their work, during the crack growth, the stress at the crack tip is equal to the ultimate stress of aluminum alloys. Fetta *et.al.* [10] showed that for small crack lengths, R curve depends on material properties but for the bigger crack lengths it depends on the geometry of specimen. Kulkarni *et.al.* [11] modeled the crack growth by 3D finite element. 20 nodes elements with 3 degrees of freedom and singular elements in the crack tip were used, showing good correlation between the numerical fracture toughness and experimental values carried on the thin steel sheets. Rankin [12] studied the ductile fracture in low carbon steel. He carried out a numerical analysis using Abaqus software in 2D. The crack tip was modeled by square shape elements. The obtained load–displacement curve was compared with experimental results, and a reasonably good agreement was achieved.

## CONCEPT OF FRACTURE MECHANICS

### Stress Intensity Factor (SIF)

SIF is one of the main rupture criteria in fracture mechanics. It is a global quantity which takes into account the stresses in the vicinity of crack tip. If this quantity reaches its critical value, crack initiates. The relation between the SIF and stresses in polar coordinates is as follows [13]:

$$\sigma_{ij} = \frac{k_\alpha}{\sqrt{2\pi r}} f_{ij}^{\alpha}(\theta), \tag{1}$$

Broek *et.al.* [14] were the first author to introduce a relationship between SIF and crack length:

$$K = F\sigma\sqrt{\pi a}, \tag{2}$$

$F$ is the correction factor of K, which is given in different forms by researchers. Lucas [15] has presented this factor as follows:

$$F = \frac{1.12}{\sqrt{1+4.5\frac{a}{R}}}, \tag{3}$$

Schijve [16] has presented the correction factor with an exponential function depending on $\frac{a}{R}$ and $\alpha$:

$$F = \frac{1}{\sqrt{2}} - \left(1.12 - \frac{1}{\sqrt{2}}\right) \exp\left(-\alpha\frac{a}{R}\right),$$
$$\alpha = 0.8\left(1 - 0.3\frac{a}{R} + 0.13\left(\frac{a}{R}\right)^2\right). \tag{4}$$

Also Kujawski [17] has presented $K$ as follows:

$$K = \left(1.12\,\sigma_{\max} + 0.683\frac{\partial\sigma}{\partial x}|a_{x=0}\right)\sqrt{\pi a}, \tag{5}$$

where $\sigma_{\max}$ and $\frac{\partial\sigma}{\partial x}$ are the maximum stress and the stress gradient at the notch.

### Plastic Zone at the Crack Tip

In an elastic- perfect plastic material with yielding stress ($\sigma_y$), which follows the maximum yield stress criteria, there is a plastic zone in the vicinity of the crack tip. Inside the plastic zone, there is a bearing zone which appears from the time of the crack

initiation. There is also an elastic zone outside the plastic zone which has a greater area than the plastic zone. This plastic zone, depends on the thickness of the specimen, the crack length and strain rate. Figure 1 shows the bearing, elasto-plastic and elastic zones at the crack tip.

In plane stress state, the radius of the plastic zone is:

$$r = \frac{1}{\pi}\left(\frac{K}{\sigma_y}\right)^2, \tag{6}$$

In the plane strain state, in which the stress has three components at the crack tip, the radius of the plastic zone is:

$$r = \frac{1}{3\pi}\left(\frac{K}{\sigma_y}\right)^2. \tag{7}$$

The above relations show the dependence of the plastic zone radius ($r$) with the SIF ($K$). By increasing $K$, $r$ increases by exponent 2. Also by increasing the crack length, $r$ increases [18]. Therefore, in the plane stress state by increasing the crack length, the critical SIF ($K_C$) should also increase.

By drilling the crack tip, the plastic zone at the crack tip disappears. In fact it appears in a moon croissant shape behind the hole and the bearing, and plasticity around the border of the hole expands, thus the radius of the plastic zone decreases. Two parameters, *i.e.* the hole diameter and crack length could influence the area of the plastic zone. Thus, in this paper 3 locations of hole at the crack tip with different diameters are studied.

## CRITICAL LOAD

Critical load is one of the fracture criteria. It depends on the $K_C$ criterion, the specimen thickness, as well as crack length and strain rate. Banerjee showed a linear relation between the critical load decrease and crack length increase [19]. Thus, the stopping holes with different locations and diameters could influence the critical load. The analysis of this phenomenon is carried out in this paper.

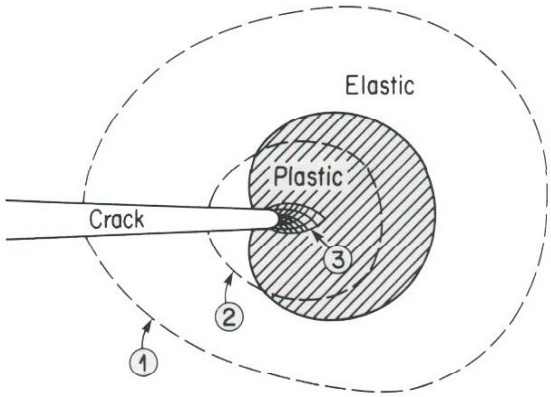


**Figure 1.** Three bearings, elasto-plastic and elastic zone in the crack tip [18].

## LOCATIONS OF THE STOPPING HOLES

Three locations as shown in Figure 2 are considered:

**Location A:** the hole is situated in the left of the crack tip,

**Location B:** it sits in the center of the crack tip,

**Location C:** it sits in the right site of the crack tip.

To study the influence of locations of the stopping holes at the crack tip, a computer model was used to found the most efficient location.

### CT Specimen

Mode I is one the most important modes of fracture [13]. To carry out a crack growth experiment in order to establish the fracture toughness of the specimen ($K_{IC}$), the standard compact tension (CT) specimen was used [20].

This specimen has an initial crack, and its dimensions are shown in Figure 3. The dimensions of the specimen used in this study are listed in Table 1. The diameters of the studied holes were 2, 4 and 6 mm which were located at positions A, B and C.

### Properties of alloy

The Al 7075-T6 alloy similar to the other alloys of Aluminum is light and resistant to oxidation. Its

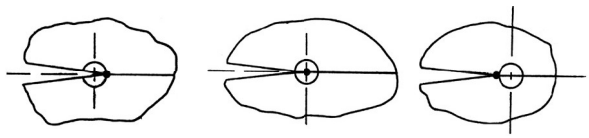


**Figure 2.** Three locations of stopping hole.

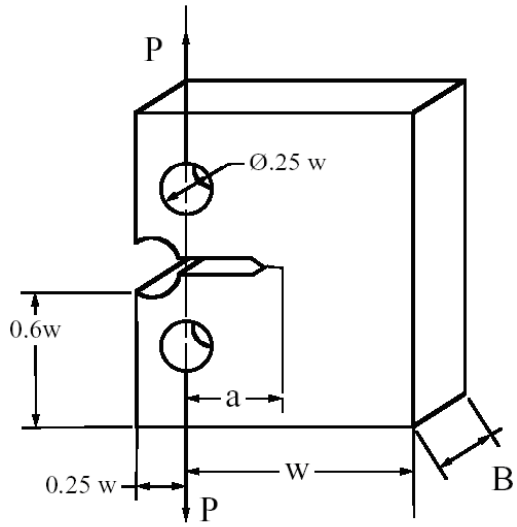


**Figure 3.** Schematics of CT specimen.

heat and electric transmission are high and suitable for machining. Also this alloy has the special properties of Aluminum of the set 7000, such as the yielding stress, hardness and thermal resistance [21].

Table 2 shows the mechanical properties of the Al 7075-T6 alloy. Due to its excellent mechanical properties and its high resistance against crack growth, this alloy has a large field of application in the aerospace industry.

## FINITE ELEMENT ANALYSIS

After modeling CT specimen by Ansys software, meshes are generated in two-dimensional (2D) and three dimensional (3D) states. In 2D modeling we used triangular elements with 6 nodes (plane 2) and in 3D modeling we used cubic elements with 20 nodes (solid 95). Both elements have 2 degrees of freedom. At the crack tip singular elements were used. Thus, the singularity of the stress at the crack tip was insured. Figure 4 shows the mesh generation at the crack tip in 2D and 3D states. In 3D modeling of the specimen with stopping hole, the meshes were refined in the vicinity of the hole, as shown in Figure 5. Dimensions of these elements were such that both the results and the error converged to constant values. Because of the symmetry of the CT specimen, only half of the specimen was modeled, and boundary conditions of symmetry were applied in the model. The boundary conditions relative to the symmetry are shown in Figure 6. Displacements of the node at either side of the crack tip were closed in all directions.

The concentrated load was applied in the node situated above the hole (Figure 6). In the experimental model, a pin translates the load to the specimen from this hole. The load was applied progressively in ten steps.

The numerical analysis was to resolve the equation using Newton-Raffson method. The curve of stress-strain of the alloy was considered by entering different points. Figure 7 shows the curve of stress-strain of the alloy:

**Table 1.** Dimensions of the CT specimen [20].

| | |
|---|---|
| W (width of specimen) | 180 mm |
| B (thickness of specimen) | 2.5 mm |
| a (crack length) | (63~83) mm |

**Table 2.** Mechanical properties of the Aluminum alloy [21].

| | |
|---|---|
| $\sigma_y$ | 510 MPa |
| $\sigma_u$ | 568 MPa |
| E | 71 GPa |
| $\nu$ | 0.33 |
| $K_{IC}$ | 30 MPa $\sqrt{m}$ |

Table 3 shows experimental results of the critical load and the critical stress intensity versus crack length [21]. In our numerical analysis, the loads given on this table were used. Then the computed stress intensity

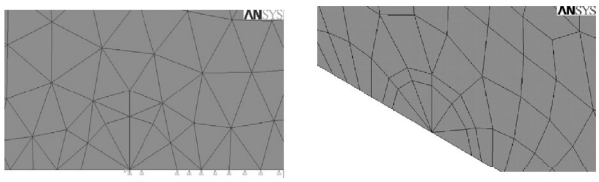


**Figure 4.** Singular elements in the crack tip (a) in 2D state (b) in 3D state.

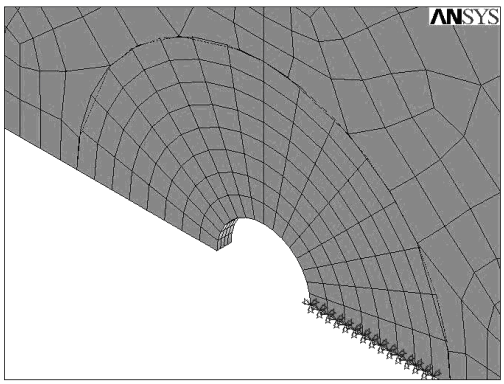


**Figure 5.** Elements in around of the stopping hole.

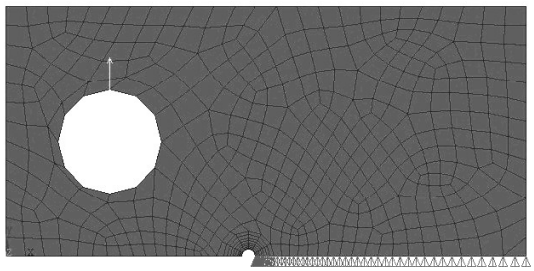

**Figure 6.** Boundary conditions and loading applied to the CT specimen.

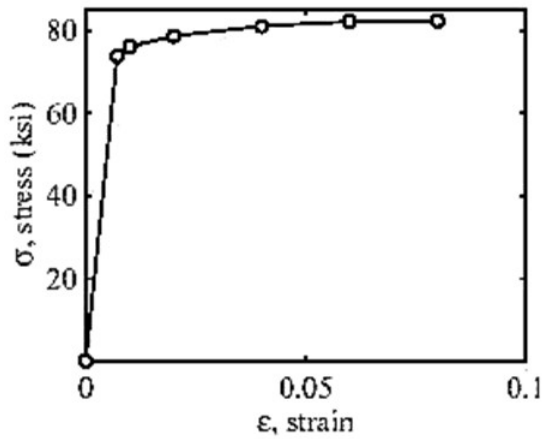


**Figure 7.** Stress-strain curve of Al 7075-T6 alloy [9].

factors in 2D and 3D states were compared with results of this table.

## NUMERICAL RESULTS

After analyzing CT specimen without a stopping hole, in which the applied critical loads were taken from experiments, the von Mises stresses in 2D and 3D states were computed. The values were between the yield stress and ultimate stress of the material, in this state, the crack growth. The values of $K_C$ in respect of the critical load were given by the software.

Figure 8 shows stress distribution which has a bean shape at the crack tip. They were used to compute the values of the critical stress intensity factor, $K_C$, versus non dimensional crack length $\left(\frac{a}{w}\right)$ which are shown in Figure 9 and compared with experimental results. Experimental conditions are described later in the paragraph relative to the experimental results.

The results show that $K_C$ increases during crack growth. Also they show that 3D analysis has more precision than 2D analysis. In 2D state, the error was 12% and in 3D it was 5%.

For computing critical load of the specimen with stopping holes, the criterion was to reach the ultimate stress of aluminum. Figure 10 shows the von Mises stress around the hole. We observe that the area of the plastic zone in specimen with a hole is greater compared to the specimen without a hole.

In the analysis of the CT specimen with stopping holes, the critical loads are given in Table 3, which was used to compute the stress intensity factors to be compared with the values of specimen without stopping

**Table 3.** Experimental results of test [21].

| a (mm) | 63 | 67 | 71 | 75 | 79 | 83 |
|---|---|---|---|---|---|---|
| $P_{cr}$ (KN) | 12.4 | 12 | 11.55 | 11.1 | 10.7 | 10.3 |
| $K_C$(MPa$\sqrt{m}$) | 91 | 92.1 | 93.6 | 94.8 | 95.2 | 96 |

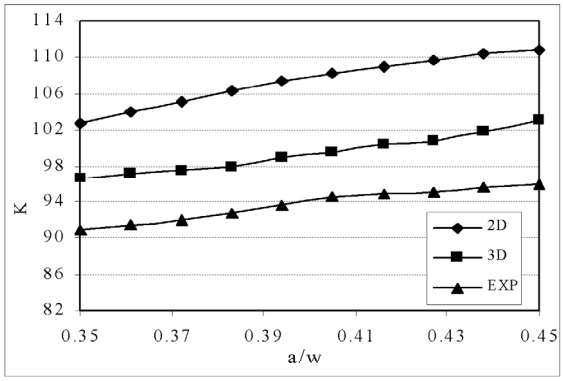


**Figure 9.** Curve of $K_C$ versus a/w in the specimen without hole in 2D and 3D states and their comparison with experimental results.

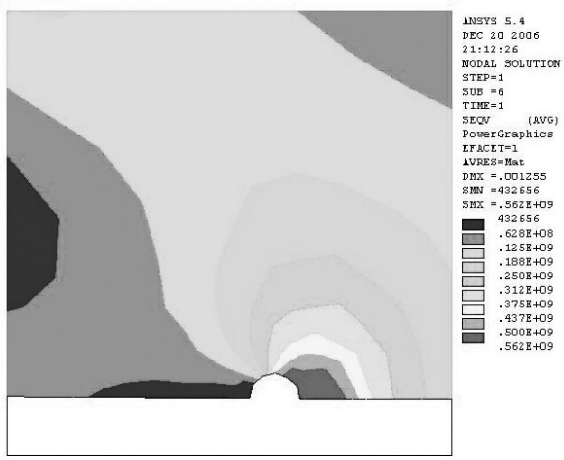


**Figure 10.** Von Mises stress around the stopping hole.

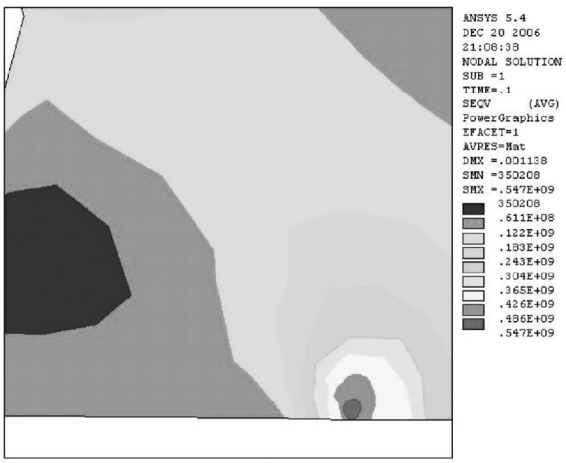


(a)

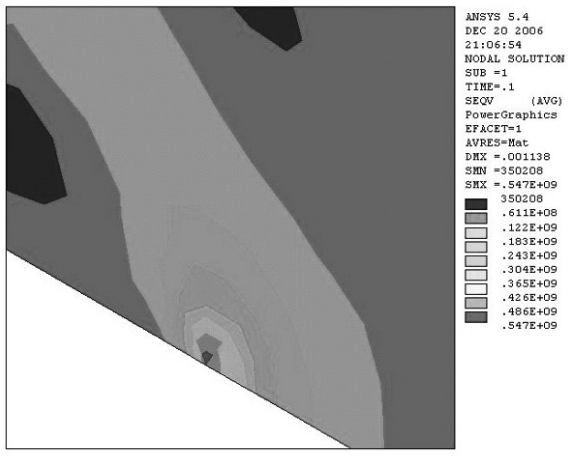


(b)

**Figure 8.** Von Mises stress at the crack tip (a) in 2D state (b) in 3D state.

holes. The results were compared in commune curves in the Figures (11-13).

$K_C$ was evaluated for the hole diameters of 2, 4 and 6 mm, and for three locations A, B and C versus non dimensional crack lengths. We observed that the computed stress intensity factors compared to $K_C$ corresponding to the specimen without stopping hole, had decreased. In the comparison, except for the existence of a hole, all of the parameters were the same. Figures (11-13) show the variation of $K_C$ relative to $(\frac{a}{w})$ in different states.

Also the percentage of decrease of $K_C$ relative to the specimen without holes is shown in Table 4 in which the mean values of crack lengths were considered.

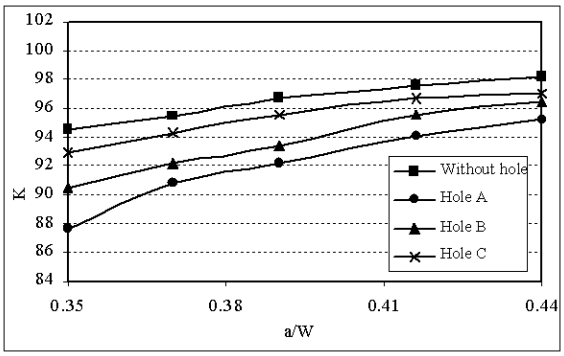


**Figure 11.** Curve of $K_C$ versus (a/w) in three locations A, B and C with hole diameter of 2mm.

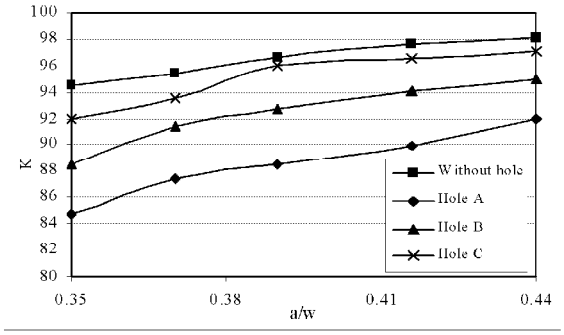


**Figure 12.** Curve of $K_C$ versus (a/w) in three locations A, B and C with hole diameter of 4mm.

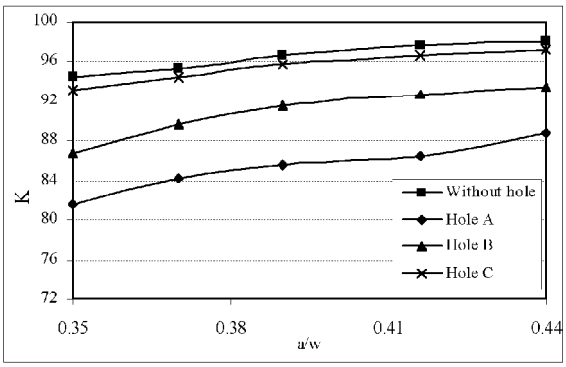


**Figure 13.** Curve of $K_C$ versus (a/w) in three locations A, B and C with hole diameter of 6mm.

Following the results, location A with a hole diameter 6mm was the best because it delayed the crack growth. Location C with a hole diameter 2mm was the worst location.

After analyzing $K_C$, we also analyzed $P_{cr}$ which was another parameter of rupture. The loads of the specimen with a stopping hole were compared with the $P_{cr}$ of the specimen without a hole. Figures (14-16) show the variation of $P_{cr}$ versus $\frac{a}{w}$. Also the percentage of decreasing $P_{cr}$ relative to the specimen without hole is shown in Table 5.

The above results show increase of $P_{cr}$ in specimen with a hole in all of the hole locations with all of

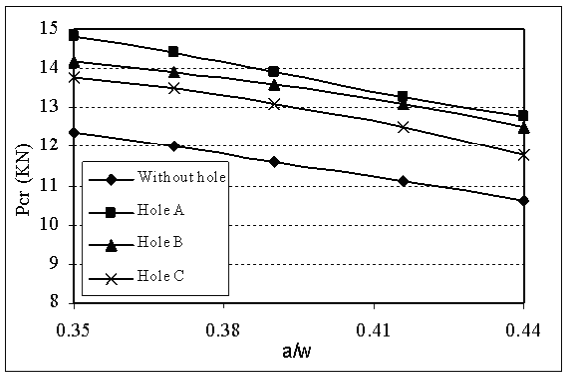


**Figure 14.** Curve of $P_{cr}$ versus a/w for three locations A, B and C with a hole diameter of 2mm.

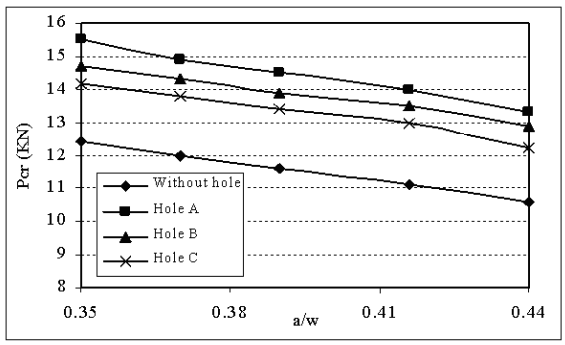


**Figure 15.** Curve of $P_{cr}$ versus a/w for three locations A, B and C with a hole diameter of 4mm.

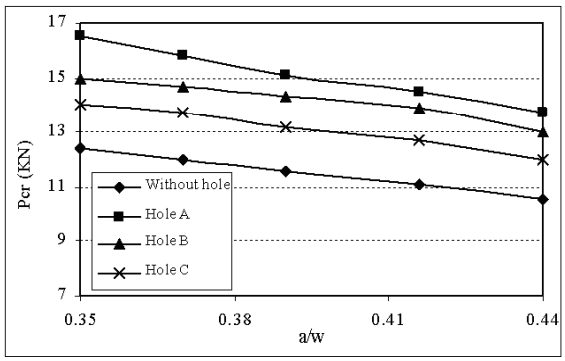


**Figure 16.** Curve of $P_{cr}$ versus a/w for three locations A, B and C with a hole diameter of 6mm.

the studied 2, 4 and 6mm diameters compared to those without a hole.

## EXPERIMENTAL RESULTS

CT specimens were made of Al 7075-T6. One such specimen is shown in Figure 3 with dimensions as given in Table 2. Specimens were made without stopping or with stopping holes in three locations with Ø6 mm. Two specimens for each location of hole were tested. As the results of both specimens for each system were similar, we did not test more specimens. The tests were carried out on a tensile machine type Amsler with a load capacity of 6 tones. Since the load was transmitted by axles, a rotation of cantilever sides was possible. We chose a low crosshead speed: 0.5 mm/min and worked at 23°C and 65% RH. The opening of the specimen was followed by displacement of the crosshead in mm scale. A special cold light lamp illuminated the sample, so the crack appeared very clearly during the experiment. Thus, we measured the critical load ($P_{cr}$) for crack initiation. Results are shown in Figure 17.

We observe that the critical load which is 12.1 KN for the specimen without a stopping hole, increases to 13.4 KN for a test bar with a stopping hole in location C, it increases to 16.1 KN in location B and to 18.6 KN in location A. Thus, location A of the stopping hole increases the critical load by about 54%, and location C increases the critical load by about 11%. Location B has an intermediate result of 33%. These results confirm the numerical one. Figure 18 shows test specimens after loading. We can observe that the plastic zone is clear in the crack tip and in test samples with a hole, it has the highest area in location C.

## CONCLUSIONS

- By increasing the non-dimensional length of the crack $(\frac{a}{w})$, $K_C$ increases. All locations A, B and C of the stopping holes, 2D and 3D analysis and experiments confirmed this phenomenon.
- Results of 3D analysis show more precision than those the 2D analysis. Therefor, in the analysis of specimen with stopping holes, 3D analysis is used.
- The curves of $K_C$ and $P_{cr}$ versus $(\frac{a}{w})$ show that in location A of the hole, by increasing the hole diameter, $K_C$ decreases and $P_{cr}$ increases. Thus, both parameters agree in stopping the crack growth.
- In location B, by increasing the hole diameter, again both parameters took a good way, but not enough as in location A. The percentage of variations presented in Table 3, confirm it. In location C of the hole which shows the weakest results to stop the growth of the crack, after diameter 4mm of the hole, the results became inverse. Table 4 shows that $K_C$ decreases, and Table 5 shows the stabilization of the $P_{cr}$. Therefore, this location of the stopping hole should not be used.

**Table 4.** Percentage of decreasing of $K_C$ versus (a/w) for different locations and diameters of hole.

| | $\phi = 2mm$ | $\phi = 4mm$ | $\phi = 6mm$ |
|---|---|---|---|
| A | %5.6 | %8.7 | %14.3 |
| B | %3 | %5.5 | %7.2 |
| C | %1.5 | %2.2 | %1.8 |

**Table 5.** Percentage of decreasing $P_{cr}$ versus a/w for different locations and diameters of a hole.

| | $\phi = 2mm$ | $\phi = 4mm$ | $\phi = 6mm$ |
|---|---|---|---|
| A | %21 | %32 | %45 |
| B | %13 | %19 | %28 |
| C | %8 | %11 | %11 |

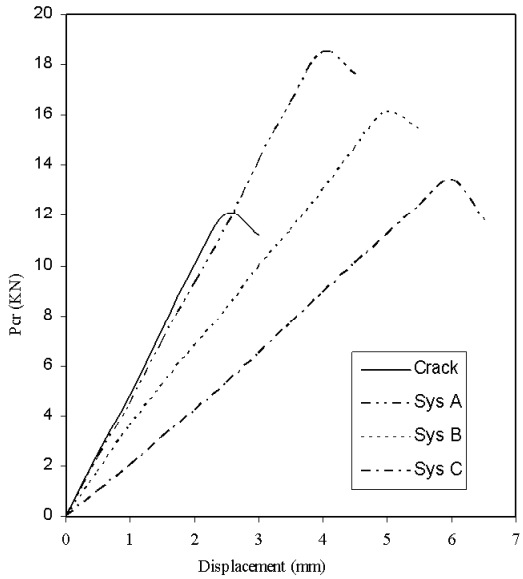


**Figure 17.** Curve of $P_{cr}$ versus displacement for the specimen without a hole and three locations A, B and C of hole Ø6mm.

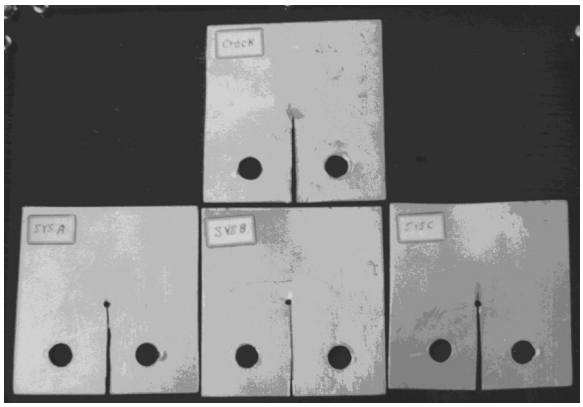

**Figure 18.** CT test bars after loading, (Above: without a hole, below from left to right locations A, B and C of the hole)

## REFERENCES


1. Natoriesh T., Asaoka T. and Inada I. , "Repair Practice of Steel Bridges", *Yokogawa Bridge Works*, PP 63-90(1992).
2. Ichikawa A., "Problems in Maintenance of Railway Steel Structures and Examples of Retrofitting and Reinforcement", *Bridge and Foundation Engineering*, **28**(8), PP 17-21(1994).
3. Finney J.M., "Service Bulletin Defines the Requirements to Perform a One-Time Visual Inspection for the Purpose of Locating Cracks in the Firewall", *Report No DSTO-TR-0434*, (2000).
4. Goodrich B.F., "Cessna Citation Brake Stators, Service Difficulty Alert", transport Canada, (2002).
5. Qi D.M., "Stop and Balancing Holes for the Improvement of Structural Integrity", M.Sc. Thesis, Cranfild Institute of Technology(1986).
6. Dirikolu M.H. and Aktash A., "Analytical and Finite Element Comparisons of Stress Intensity Factors of Composite Materials", *Composite Structures*, **50**, PP 99-102(2000).
7. Finney J.M. and Niessen J., "Repair of Plastic Plate and Sheet", *DSTO Technical Report 0434*, (1998).
8. Callinan R.J., Wang C.H. and Sanderson S., "Analysis of Fatigue Crack Growth From Cold-Expanded/Interference Fitted Stop Drilled Holes", *DSTO Technical Report 0704*, (1998).
9. Chen C.S., Wawrzynek P.A. and Ingraffea A.R., "Crack Growth Simulation and Residual Strength Prediction in Airplane Fuselages", *Report NASA/CR-1999-209115*, Cornell University, New York, NASA/CR, (1999).
10. Fetta T., Munz D., Geraghty R.D. and White K.W., "Influence of Specimen Geometry and Relative Crack Size on R-Curve", *Engineering Fracture Mechanics*, PP 375-386(2000).
11. Kulkarni D.M., Prakash R. and Kumar A., "Experimental and Finite Element Analysis of Fracture Criterion in General Yielding Fracture Mechanics", *Engineering Fracture Mechanics*, **27**, PP 631-642 (2002).
12. Rakin M., "Numerical Modeling of Ductile fracture Initiation in Structural Steel", *Engineering Fracture Mechanics*, **11**, PP 934-946(2001).
13. Francois D., Pineau A. and Zaoui A., *Comportement Mecanique Des Materiaux*, 3Ed., Hermes, (1993).
14. Broek D. and Vliegar H., "The Propagation of Fatigue Cracks Emanating From Hole", *International Journal of Fracture*, **11**(2), PP 283-294(1972).
15. Lucas P., "Stress Intensity Factors of Small Cracks at Holes", *Engineering Fracture Mechanics*, **26**, PP 471-473(1987).
16. Schijve J., "The Stress Intensity Factor of Small Cracks at Notches", *Fatigue and Fracture of Engineering Material and Structure*, **5**, PP 77-90(1982).
17. Kujawski D., "Estimation of Stress Intensity Factor for Small Cracks at Notches", *Fatigue and Fracture of Engineering Material and Structure*, **14**, PP 953-965(1991).
18. Li H., "Analysis of Crack Growth and Crack Tip Plasticity in Ductile Materials Using Cohesive Zone Models", *International Journal of Plasticity*, **19**, PP 849-882(2003).
19. Banerjee S., "Size and Geometry Effects", *6th International Conference of Fracture*, New Dehli, India , (1984).
20. Davis J.R., *Aluminium and Aluminium Alloys*, 4Ed., ASM Specialty Handbook, PP 648-649(1999).
21. Annual book of ASTM standard, *Metals Test Methods and Analytical Procedures*, ASTM Publications, PP 522-557 (1993).